Plasmonics
https://doi.org/10.1007/s11468-025-03001-8

RESEARCH

Plasmon-Enhanced ZnO/Ag Nanoparticles with Synergistic Antibacterial and Anticancer Activities

Shaymaa Awad Kadhim[1] · Rusul A. Ghazi[2] · Ali Abbasi[3] · Mohammad Waleed M. Sadaka[4] · Forat H. Alsultany[5] · Maryam Hakim Flayih[6] · Ameer F. Shamkhi[7]

Received: 22 February 2025 / Accepted: 29 April 2025
© The Author(s), under exclusive licence to Springer Science+Business Media, LLC, part of Springer Nature 2025

Abstract

Plasmonic nanomaterials have garnered significant attention for their enhanced optical, antibacterial, and anticancer properties, owing to their surface plasmon resonance (SPR) effects. In this study, ZnO and ZnO/Ag nanoparticles were synthesized using green synthesis approach. The structural, morphological, and physicochemical properties of the fabricated nanomaterials were systematically characterized via X-ray diffraction (XRD), Fourier-transform infrared spectroscopy (FT-IR), transmission electron microscopy (TEM), and dynamic light scattering (DLS). XRD analysis confirmed the hexagonal wurtzite structure of ZnO, while additional peaks in ZnO/Ag nanoparticles indicated successful silver incorporation. TEM imaging revealed a spherical morphology with average particle sizes of 35 ± 10 nm for ZnO and 55 ± 10 nm for ZnO/Ag. The antibacterial activity of the nanoparticles was assessed against *Klebsiella pneumoniae*, *Pseudomonas aeruginosa*, *Escherichia coli*, *Streptococcus mutans*, *Staphylococcus aureus*, and *Enterococcus faecalis* using broth microdilution method. ZnO/Ag nanoparticles exhibited superior antibacterial efficacy, particularly against Gram-negative strains, due to the synergistic action of ZnO-mediated oxidative stress and Ag^{+}-induced membrane disruption. The plasmonic properties of Ag further contributed to the antibacterial effect by enhancing reactive oxygen species (ROS) generation under light exposure. Moreover, the MTT assay demonstrated a dose-dependent cytotoxic effect on A-549 lung carcinoma cells, with ZnO/Ag nanoparticles displaying a lower IC50 than ZnO. The enhanced anticancer activity was attributed to increased mitochondrial dysfunction, ROS generation, and apoptosis induction, further amplified by plasmonic interactions. These findings highlight the potential of ZnO/Ag nanomaterials as promising candidates for biomedical applications, particularly in antimicrobial and anticancer therapies.

Keywords Plasmonic effect · ZnO/Ag nanoparticles · Antibacterial · Anticancer · Silver · A-549

Introduction

In recent decades, nanoscience and nanotechnology have emerged as advanced and highly applicable fields in diverse areas such as energy [1], medicine [2], pharmaceuticals [3], and consumer products. Among these, nanotechnology-based therapies are increasingly recognized as promising strategies for tackling critical health challenges like cancer and antimicrobial resistance [4–6].

Cancer remains one of the leading causes of death worldwide. It is characterized by genetic mutations that disrupt normal cellular function and trigger uncontrolled proliferation and tumor formation [7]. Traditional treatments such as chemotherapy and radiotherapy, although widely used, often result in severe side effects that compromise patient quality of life [8]. Consequently, researchers are seeking alternative approaches that enhance therapeutic efficacy while

✉ Ali Abbasi
Ali.abbasi@hu.edu.iq

1 Department of Physics, Faculty of Science, University of Kufa, Al-Najaf, Iraq

2 Physics Department, College of Science, University of Babylon, Babylon, Iraq

3 College of Pharmacy, Al-Hadba University, Mosul, Iraq

4 Department of Medical Biochemical Analysis, Cihan University-Erbil, Erbil, Kurdistan Region, Iraq

5 Department of Medical Physics, College of Sciences, Al-Mustaqbal University, 51001 Babylon, Iraq

6 Department of Physics, Faculty of Science, University of Kufa, Kufa, Iraq

7 Department of Physics, Faculty of Science, University of Kufa, Kufa, Iraq

Published online: 11 June 2025

reducing adverse effects. One such promising avenue is the application of nanotechnology in cancer therapy, particularly through the use of nanomaterials [9, 10].

This study aims to develop and characterize nanoparticles with enhanced anticancer activity. Among various nanomaterials, zinc oxide (ZnO) nanoparticles are particularly appealing due to their low toxicity, ease of synthesis, and multifunctionality [11–13]. These properties have enabled their integration into gas sensors [14], solar cells [15], and biomedical applications [16].

Recent findings suggest that combining metal oxides like ZnO or TiO_2 with noble metals such as silver or gold can significantly enhance their biological performance [17–19]. For example, Ghoreishi et al. reported that hybrid ZnO–Au nanoparticles exhibited superior anticancer properties compared to ZnO alone [20].

Plasmonic metal nanoparticles such as silver (Ag) and gold (Au) exhibit surface plasmon resonance (SPR), which can profoundly influence their optical, electronic, and biological characteristics [21]. SPR enhances light absorption and electron excitation, boosting photocatalytic and biomedical performance [22–24]. In ZnO/Ag systems, this coupling is especially advantageous, as it increases reactive oxygen species (ROS) generation and promotes antibacterial and anticancer activities via mechanisms like membrane disruption and apoptosis induction [25, 26].

Various synthesis techniques have been employed to tailor the properties of such nanomaterials [27, 28]. Katouah et al. utilized thermal decomposition to prepare ZnO nanoparticles, followed by biological assessments [29]. Mahmoudi Khatir et al. adopted the sol–gel method to synthesize Cu-doped ZnO nanoparticles with significant bioactivity [30]. However, many of these methods involve hazardous chemicals that raise concerns about safety and environmental sustainability.

To address these concerns, green synthesis techniques using plant extracts have gained traction. These eco-friendly methods are cost-effective, scalable, and environmentally sustainable [31]. For instance, Guo et al. used almond gum to synthesize bismuth oxide nanoparticles and investigated their environmental compatibility [32]. In the past decade, various extracts were used for synthesis of nanomaterials like *Fophora flavescens* [33], *Ficus carica* [34], *Crataegus monogyna* [35], *Sophora flavescens* [36], *Tangerine* peel [37], and *Mentha pulegium* [38]. Considering the growing interest in plasmonic nanomaterials, integrating Ag into ZnO nanoparticles could yield multifunctional systems with enhanced optical and biological capabilities. Such hybrid nanostructures can improve light-matter interactions and facilitate charge transfer, offering great potential for next-generation antimicrobial and anticancer applications [31].

In contrast to conventional synthesis methods, this study introduces a green, eco-friendly approach for the fabrication of ZnO/Ag nanoparticles using *Vicia faba* stem extract as a novel biogenic reducing and stabilizing agent. The resulting nanoparticles exhibit not only superior antibacterial properties but also notable anticancer activity against lung carcinoma cells. This dual-functional behavior, combined with a sustainable synthesis route, positions our work at the intersection of green chemistry and biomedical innovation, offering a distinctive contribution to the field of plasmon-enhanced nanomaterials.

Experimental

Materials

The following chemicals were utilized in this study: silver nitrate ($AgNO_3$, $\geq 99.0\%$), sodium dodecylbenzenesulfonate (SDBS), absolute ethanol ($\geq 99.9\%$), and zinc nitrate hexahydrate ($Zn(NO_3)_2{\cdot}6H_2O$), all of which were procured from Sigma-Aldrich. Deionized water was used as the primary solvent for the nanoparticle synthesis. Moreover, the MTT reagent (3-(4,5-dimethylthiazol-2-yl)−2,5-diphenyltetrazolium bromide) was purchased from Merck.

Extract Preparation

The extraction process began with the careful selection and identification of *Vicia faba* stems by an expert botanist. Fresh stems were repeatedly washed with distilled water to remove any adhering dust or contaminants. They were then air-dried in a shaded environment for 8 days, ensuring that their beneficial compounds remained intact. Once dried, the stems were finely ground into a powder using a mechanical grinder. To extract the bioactive compounds, 50 g of this powdered plant material was immersed in deionized water and heated on a hot plate at 75 °C for 30 min. As the solution was heated, its color gradually changed, indicating the release of phytochemicals. The mixture was then carefully filtered using Whatman No. 1 filter paper. The resulting extract was transferred to a refrigerator at 4 °C for storage, where it remained stable until further use in nanoparticle synthesis.

Fabrication of Zinc Oxide Nanoparticles

The fabrication of zinc oxide nanoparticles followed a modified standard protocol aimed at optimizing nanoparticle uniformity. The process began with dissolving 1 g of zinc nitrate in 15 mL of deionized water while stirring vigorously at room temperature. To enhance particle homogeneity, SDBS was used as a stabilizing agent. A separate SDBS solution (20 mL at 40 °C) was prepared, maintaining a 1:1 ratio with zinc nitrate, and was carefully added to the reaction vessel. After 30 min of continuous stirring,

the pH was gradually raised to 12 by adding ammonia solution dropwise. This step facilitated the formation of a zinc hydroxide precipitate, which was left to react for 90 min. The precipitate was then separated via centrifugation, washed thoroughly three times with deionized water to remove any impurities, and dried. Finally, the dried product was subjected to calcination at 650 °C for 2 h, yielding pure ZnO nanoparticles with improved crystallinity.

Biosynthesis of ZnO/Ag Nanoparticles

In this process, the *Vicia faba* stem extract obtained earlier was used to reduce silver ions, facilitating the formation of Ag NPs on the ZnO NPs. The method was based on Kiani et al.'s approach [39], with slight modifications in pH regulation and extract concentration to optimize the synthesis. To ensure a uniform dispersion of ZnO nanoparticles and prevent agglomeration, 0.4 g of ZnO was first treated with ultrasonication for 1 h. In a separate step, silver nitrate was dissolved in 8 mL of deionized water, maintaining a 10% molar ratio with respect to ZnO. This solution was gradually introduced into the ZnO suspension under continuous stirring. Then, 10 mL of *Vicia faba* stem extract, previously adjusted to pH 12 with sodium hydroxide, was slowly added to the reaction vessel. The reaction proceeded for 1 h, during which silver ions were reduced, forming ZnO/Ag hybrid nanoparticles. The final precipitate was collected, thoroughly washed to remove residual impurities, and dried. The synthesized ZnO/Ag nanostructures were then prepared for biological applications, leveraging their potential antimicrobial and catalytic properties.

Determination of Antibacterial Performance

The antibacterial activity was evaluated using the microdilution technique, which allows for the determination of the effectiveness of ZnO, ZnO/Ag nanoparticles, and *Vicia faba* stem extract against bacterial strains. In this method, 100 µL of each sample, prepared at varying concentrations, was added to the test wells. To each well, 100 µL of bacterial suspension was introduced. After incubation, the presence or absence of bacterial growth was visually assessed by examining turbidity, and the minimum inhibitory concentration (MIC) was identified as the lowest concentration that inhibited visible growth. The bacterial strains used in this experiment included *Pseudomonas aeruginosa*, *Klebsiella pneumoniae*, *Staphylococcus aureus*, *Streptococcus mutans*, *Escherichia coli*, and *Enterococcus faecalis*.

Evaluation of Anticancer Performance

To assess the anticancer potential of ZnO and ZnO/Ag nanoparticles, their cytotoxic effects were evaluated against the A-549 lung cancer cell line. The experimental approach was adapted from Zare-Bidaki et al., with slight modifications to optimize the conditions [40]. First, A-549 cells were cultured in a growth medium containing fetal bovine serum (FBS) and streptomycin to support cell proliferation. Once the cells reached 80% confluency, they were detached using 1% trypsin and prepared for further testing. The MTT assay was used to evaluate cell viability. In this assay, 10,000 cells per well were seeded into a 96-well plate. After a period of incubation, the old medium was replaced with a fresh ZnO and ZnO/Ag nanoparticle suspensions at concentrations of 12.5, 25, 50, 100, 200, and 400 µg/mL. Following another incubation, the medium was replaced with a 10% MTT solution, which allows viable cells to convert the reagent into formazan crystals. After further incubation, the supernatant was carefully removed, and the formazan crystals were dissolved in DMSO. Finally, the optical density at 570 nm was measured, and cell viability at different concentrations was calculated using the relevant formula.

$$\text{Cell viability (\%)} = (\text{Absorption of nanoparticles}/\text{Absorption of control}) * 100$$

Results and Discussion

X-Ray Diffraction

The XRD analysis was conducted to investigate the crystalline nature and phase composition of the synthesized ZnO and ZnO/Ag nanoparticles, which were prepared using *Vicia faba* stem extract. The diffraction patterns are presented in Fig. 1. As shown in Fig. 1a, the XRD pattern of ZnO nanoparticles exhibited characteristic peaks at 2θ values of 31.56°, 34.37°, 36.02°, 46.94°, 55.84°, 62.36°, 66.21°, and 69.11°, corresponding to the (100), (002), (101), (102), (110), (103), (200), and (201) planes. These results confirm the hexagonal wurtzite structure of ZnO, as indexed in JCPDS card no. 01–080-0075, and are consistent with the findings of Mohammadi-Aghdam et al., who synthesized

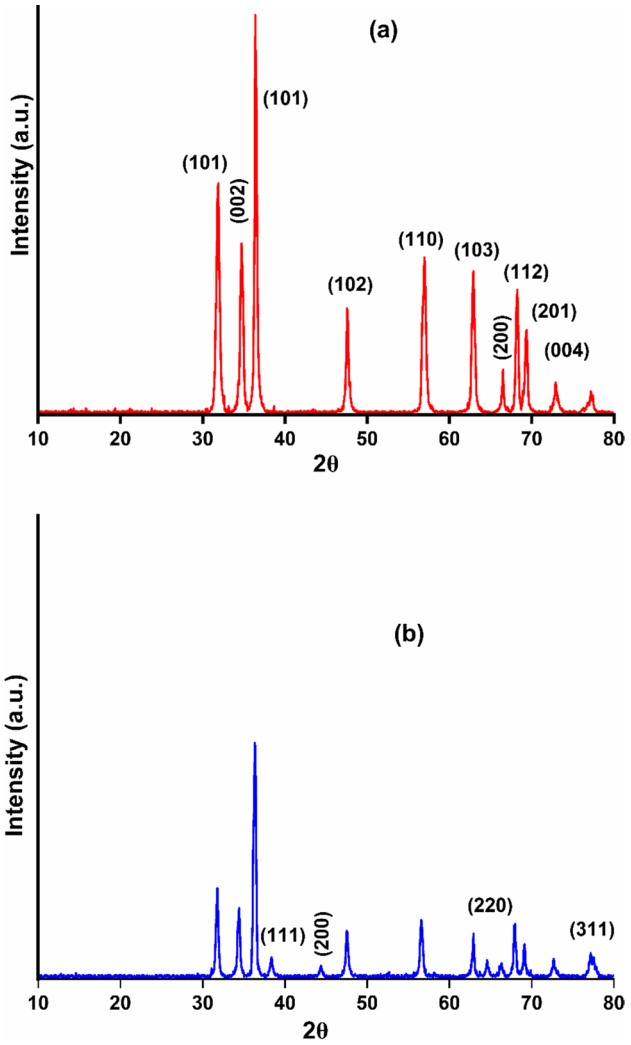

Fig. 1 XRD patterns of (**a**) pure ZnO and (**b**) biosynthesized ZnO/Ag nanoparticles using *Vicia faba* stem extract at room temperature

ZnO nanoparticles using *Hedera colchica* extract [41]. After silver ion reduction on ZnO nanoparticles using *Vicia faba* stem extract, the XRD pattern of the ZnO/Ag nanoparticles revealed four additional peaks at 38.41°, 44.64°, 64.57°, and 76.81° (Fig. 1b), which correspond to the (111), (200), (220), and (311) planes of silver nanoparticles, respectively. The absence of extra peaks suggests a highly pure ZnO/Ag structure without detectable impurities. These results are in agreement with Kiani et al., who reported similar diffraction peaks (38.2°, 42.1°, 64.7°, and 77.1°) for ZnO/Ag nanoparticles synthesized using *Lavandula stoechas* extract and deposited onto ZnO [17]. The presence of silver peaks alongside those of ZnO indicates that Ag was successfully incorporated without altering the crystal structure of ZnO. Although no clear shift in ZnO peaks was observed, the addition of Ag may introduce slight lattice strain or surface defects at the interface, which could influence the crystallinity and electronic behavior of the material.

FT-IR Spectra

The FT-IR spectra of the synthesized ZnO and ZnO/Ag nanoparticles are shown in Fig. 2. This technique helps to identify the bonding interactions and functional groups involved in the synthesis process. As seen in Fig. 2a, two prominent peaks were detected in the ZnO spectrum. A broad absorption band around 3416 cm^{-1} corresponds to hydroxyl (-OH) groups, which may result from adsorbed moisture or water molecules present on the ZnO surface. Additionally, the Zn–O stretching vibration appears as an absorption band around 572 cm^{-1}, confirming the successful formation of ZnO nanoparticles. Following the reduction of silver ions onto ZnO nanoparticles, the Zn–O absorption intensity in the 500–600 cm^{-1} range decreased, indicating interaction between ZnO and Ag nanoparticles. Moreover, a new absorption band at 3427 cm^{-1} emerged, which is linked to O–H stretching vibrations from the plant extract. These hydroxyl groups, particularly from phenolic compounds, play a crucial role in reducing Ag^{+} ions to Ag nanoparticles. Further investigation of the FT-IR spectrum revealed additional absorption bands in the 1000–1700 cm^{-1} region, which are associated with organic compounds from the plant extract, confirming the successful formation of ZnO/Ag nanoparticles (Fig. 1b). Similar observations were reported by Siami-Aliabad et al., who synthesized ZnO/Ag nanoparticles using *Sophora pachycarpa* extract [18]. Their FT-IR spectra also displayed plant-derived functional groups, confirming that silver ions were effectively reduced and deposited onto the ZnO surface.

Morphological and Size Study

To analyze the size and shape of the synthesized ZnO and ZnO/Ag nanoparticles, transmission electron microscopy (TEM) was performed. The resulting images are displayed in Fig. 3a and b, respectively. As shown in Fig. 3a, the ZnO nanoparticles exhibit a spherical shape, with their sizes ranging from 35 ±10 nm. However, some areas reveal particle agglomeration, where multiple nanoparticles have clustered together. In the case of ZnO/Ag nanoparticles, the morphology remains spherical, but with a more clustered arrangement. This structural modification is due to the presence of silver nanoparticles, which act as metallic centers, influencing the overall morphology. The ZnO/Ag nanoparticles were found to have particle sizes within the 55 ±10 nm range (Fig. 3b). These observations align with the findings of Abou Oualid et al., who also reported cluster-like formations when silver nanoparticles were deposited onto ZnO surfaces [42].

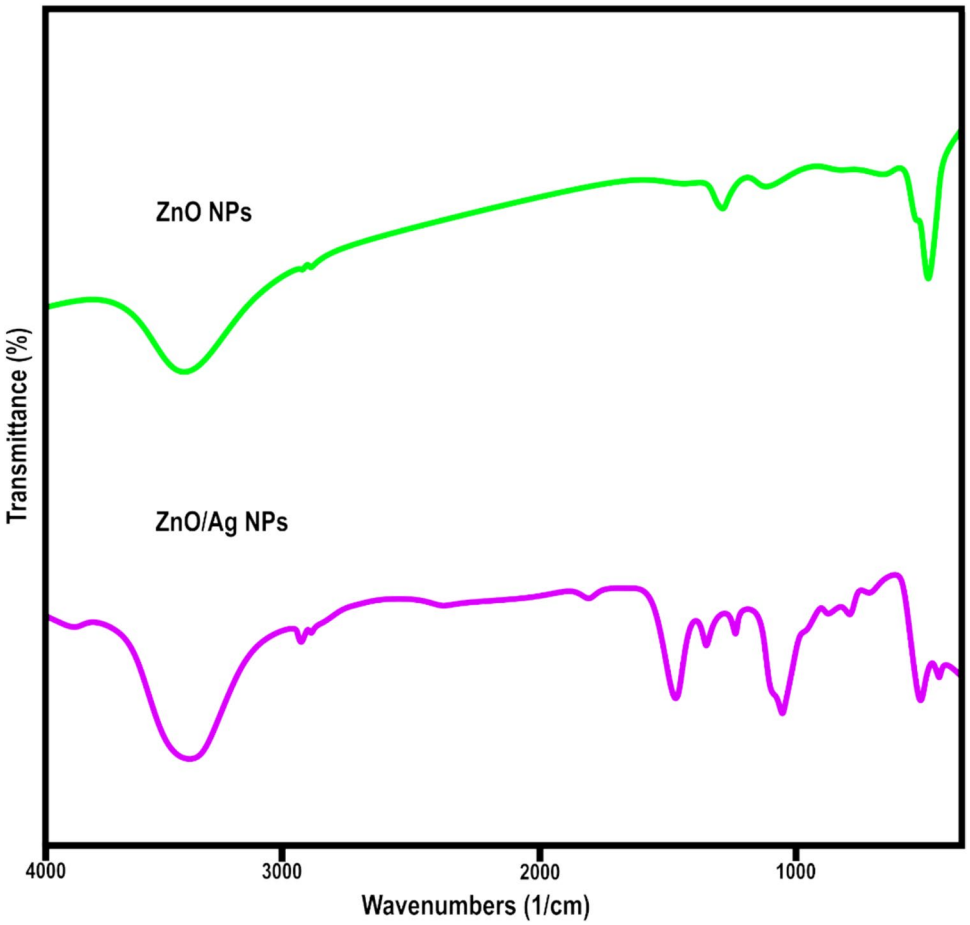

Fig. 2 FT-IR spectra of (**a**) pure ZnO and (**b**) green synthesis of ZnO/Ag nanoparticles using *Vicia faba* stem extract

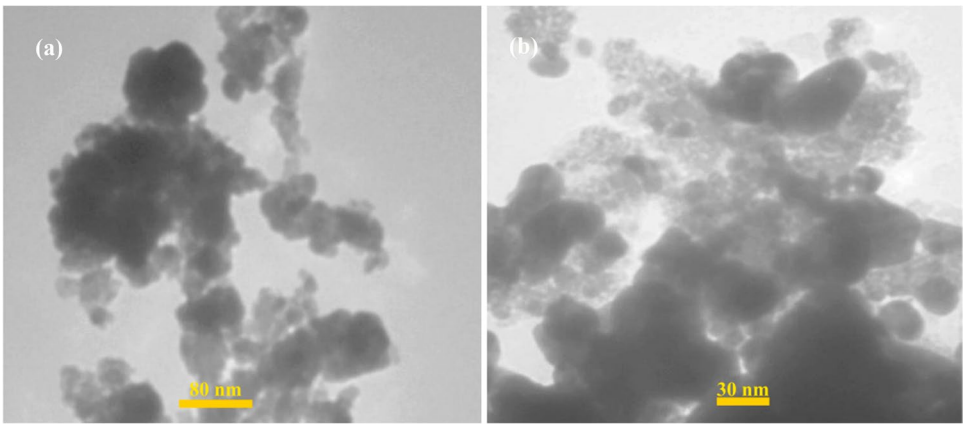

Fig. 3 Morphology and size results of (**a**) ZnO and (**b**) green synthesized ZnO/Ag nanoparticles

Hydrodynamic Diameter and Surface Charge

To assess the dispersion stability and particle size uniformity, dynamic light scattering (DLS) analysis was conducted, focusing on the zeta potential and hydrodynamic diameter of the synthesized nanoparticles. The DLS results for both ZnO and ZnO/Ag nanoparticles are illustrated in Fig. 4. The ZnO nanoparticles showed a fairly uniform size distribution, though their hydrodynamic diameter was larger than expected. This size increase was likely due to particle agglomeration, a finding that was consistent with TEM analysis. Similarly, ZnO/Ag nanoparticles also exhibited a larger hydrodynamic size, indicating some degree of particle aggregation in suspension. DLS revealed that the hydrodynamic sizes of ZnO and ZnO/Ag nanoparticles were found to range between 20–55 and 40–95 nm,

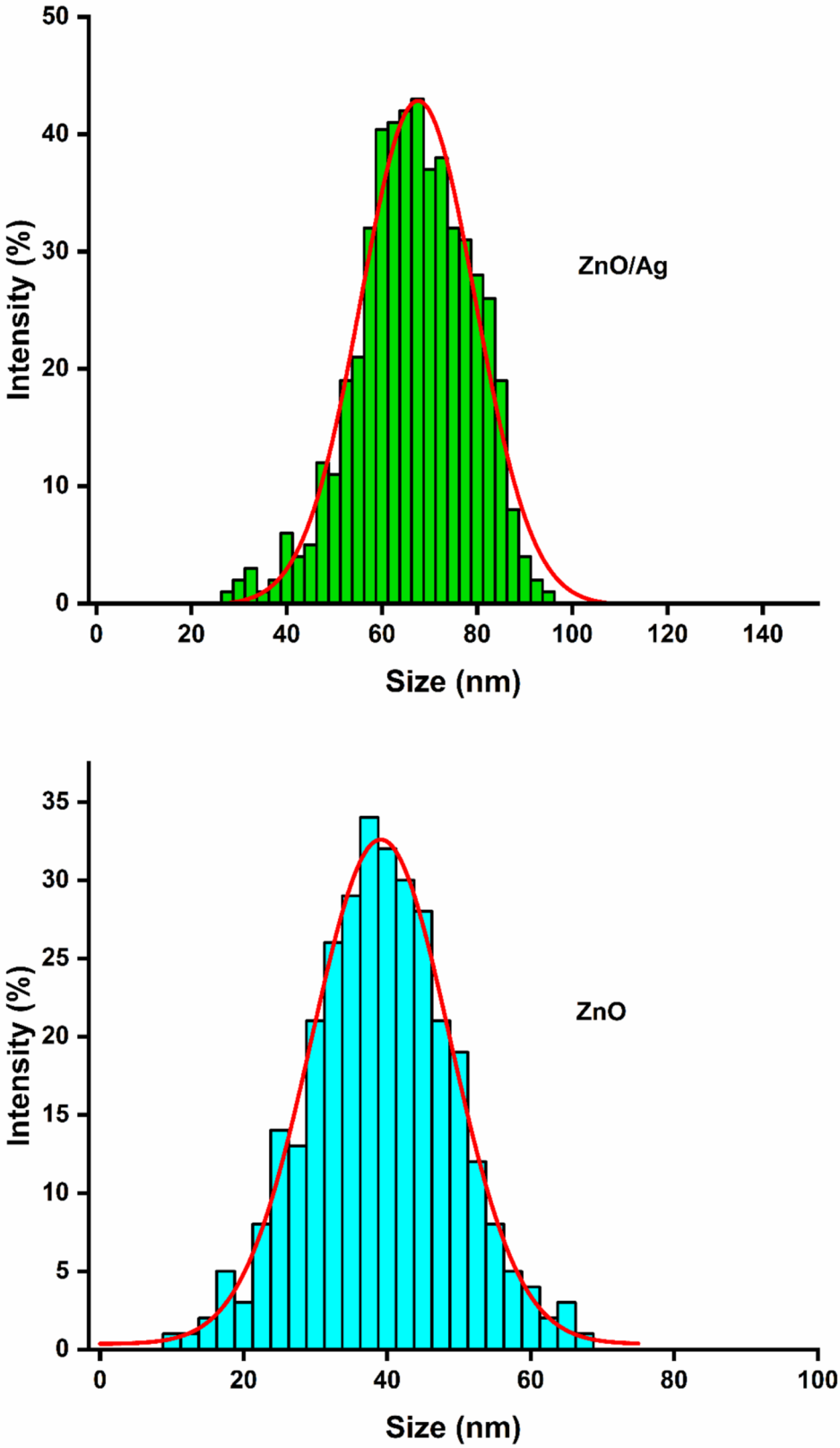

Fig. 4 Dynamic light scattering analysis of pure ZnO and green synthesized ZnO/Ag nanoparticles

respectively. Additionally, zeta potential measurements revealed values of − 3.15 mV for ZnO nanoparticles and − 7.61 mV for ZnO/Ag nanoparticles. These relatively low zeta potential values suggest that the particles experience only mild repulsive forces, which could lead to increased aggregation and larger apparent sizes in solution.

Determination of Antibacterial Performance

To investigate the antibacterial efficacy of ZnO and ZnO/Ag nanoparticles, their inhibitory effects were assessed using the broth microdilution method against six bacterial strains, including both Gram-positive and Gram-negative bacteria (Table 1). The antibacterial properties of *Vicia faba* stem extract were also analyzed, but no substantial inhibitory effects were observed, even at concentrations up to 5000 µg/mL. This aligns with the findings of Shirzadi-Ahodashti et al., who reported minimal antibacterial activity from similar plant extracts at concentrations below 4000 µg/mL [43]. The results demonstrated that ZnO nanoparticles alone exhibited moderate antibacterial effects, with MIC values of 940 µg/mL for *Streptococcus mutans*, 235 µg/mL for *Pseudomonas aeruginosa*, 470 µg/mL for *Enterococcus faecalis*, 940 µg/mL for *Staphylococcus aureus*, 235 µg/mL for *Escherichia coli*, and 470 µg/mL for *Klebsiella pneumoniae*. However, their efficacy was limited against other tested strains, suggesting that ZnO alone may not be sufficient for broad-spectrum antimicrobial applications. The incorporation of Ag nanoparticles into the ZnO matrix (ZnO/Ag) significantly enhanced antibacterial potency, with MIC values as low as 58.75 µg/mL for Gram-negative bacteria. This enhancement is primarily due to the cumulative effect of ZnO and Ag nanoparticles, which act through multiple antibacterial mechanisms. Silver ions disrupt bacterial DNA replication and protein synthesis, while ZnO nanoparticles induce oxidative stress by generating reactive oxygen species [17]. Additionally, Ag^+ ions interfere with membrane permeability and metabolic pathways, leading to bacterial apoptosis. One of the key observations in this study was the superior antibacterial efficacy of ZnO/Ag against Gram-negative bacteria, which are generally more resistant to conventional antibiotics. This increased sensitivity may be attributed to the structural characteristics of Gram-negative bacterial cell walls, which contain porins that facilitate nanoparticle penetration, making them more vulnerable to oxidative damage. The proposed mechanism of bacterial inhibition by ZnO/Ag nanoparticles is depicted in Fig. 5, illustrating their interaction with bacterial membranes, intracellular components, and oxidative stress pathways. These findings suggest that ZnO/Ag nanomaterials hold significant potential as next-generation antibacterial agents, particularly against drug-resistant bacterial strains. The antibacterial performance of the synthesized ZnO/Ag nanoparticles was compared with previous studies involving similar nanomaterials (Table 2).

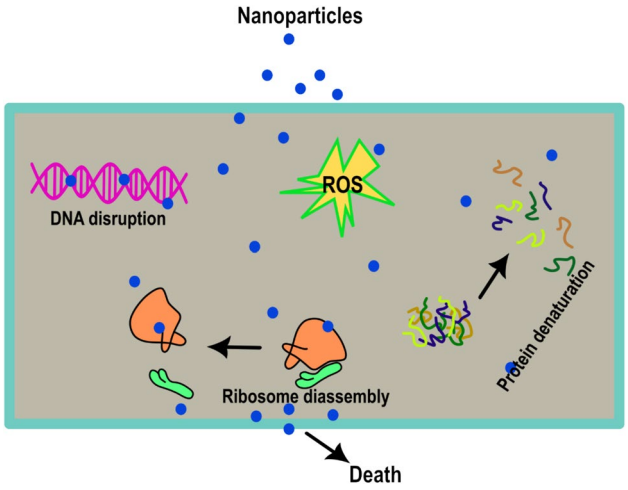

Fig. 5 Presenting a proposed mechanism for bacterial cell wall destruction using nanoparticles

Anticancer Performance of Pure ZnO and ZnO/Ag Nanoparticles

Given the physicochemical properties, dosage, and morphology of nanoparticles, the anticancer activity of ZnO and ZnO/Ag nanoparticles was investigated against A-549 lung carcinoma cells at different concentrations using the MTT assay. The results, depicted in Fig. 6, reveal a

Table 1 Antibacterial activity results of extract, ZnO, and ZnO/Ag nanoparticles synthesized using *Vicia faba* stem extract

Bacteria	Extract	ZnO NPs		ZnO/Ag NPs	
	MIC (µg/ml)	MIC (µg/ml)	MBC (µg/ml)	MIC (µg/ml)	MBC (µg/ml)
Streptococcus mutans	> 5000	940	1880	235	940
Pseudomonas aeruginosa	> 5000	235	940	58.75	235
Enterococcus faecalis	> 5000	470	1880	117.5	470
Staphylococcus aureus	> 5000	940	1880	235	940
Escherichia coli	> 5000	235	940	117.5	470
Klebsiella pneumoniae	> 5000	470	940	58.75	235

Table 2 Comparative antibacterial activity of ZnO/Ag nanoparticles

Sample	Extract used	Bacteria	MIC (µg/ml)	Ref
ZnO/Ag	*Launaea acanthodes*	*E. coli*	117.5	[39]
		S. aureus	235	
		E. faecalis	470	
ZnO/Ag	*Prosophis fracta*	*A. baumannii*	3.12	[44]
		P. aeruginosa	3.12	
ZnO/Ag	*Fenugreek*	*E. coli*	0.625	[45]
		S. aureus	1.25	
ZnO/Ag	*Pomegranate peel*	*E. faecalis*	250	[46]
		B. subtilis	15.62	
ZnO/Ag	*Hedera colchica*	*A. baumannii*	0.44	[41]
		E. faecalis	0.89	
		P. aeruginosa	7.1	

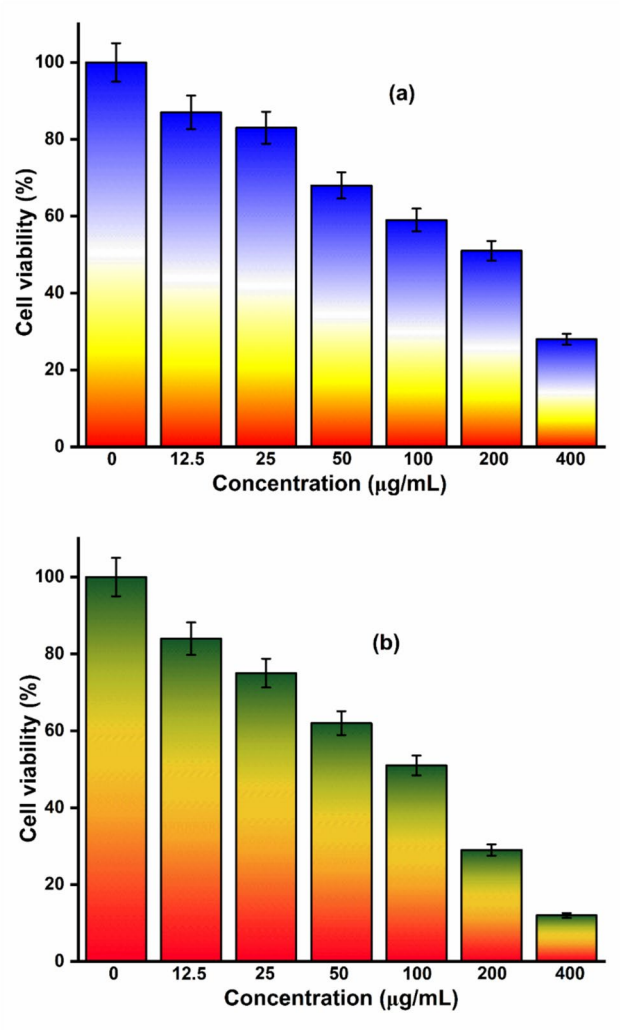

Fig. 6 Anticancer activity of ZnO and ZnO/Ag nanoparticles on A-549 lung carcinoma cells at different concentrations

dose-dependent cytotoxic effect for both types of nanoparticles. In the case of ZnO nanoparticles (Fig. 6a), cell viability decreased from 91.6% at 12.5 µg/mL to 32.4% at 400 µg/mL. However, a remarkable enhancement in anticancer activity was observed when silver nanoparticles were incorporated onto ZnO using *Vicia faba* stem extract. ZnO/Ag nanoparticles significantly reduced cell viability from 85.1% at 12.5 µg/mL to 30.7% at 200 µg/mL (Fig. 6b). The IC50 values were calculated as 165.1 µg/mL for ZnO and 77.3 µg/mL for ZnO-Ag, further confirming the increased potency of ZnO/Ag. This enhanced cytotoxic effect can be explained by the combined impact of ZnO and Ag nanoparticles on cellular structures. ZnO nanoparticles primarily induce oxidative stress by generating reactive oxygen species, which damage cellular components such as DNA, lipids, and proteins, ultimately triggering apoptosis. Silver nanoparticles, on the other hand, contribute to cytotoxicity through additional mechanisms, including disruption of cellular membranes, inhibition of essential enzymes, and interference with ATP production. The presence of silver in ZnO/Ag nanoparticles enhances cellular uptake, leading to increased bioavailability and a stronger cytotoxic response. The study also highlights the selective nature of ZnO/Ag cytotoxicity. Cancer cells, due to their altered redox homeostasis and higher metabolic activity, are more vulnerable to oxidative stress compared to normal cells. This selectivity is particularly significant in the context of targeted cancer therapy, where minimizing damage to healthy tissues is crucial. Similar findings have been reported in previous studies, where ZnO/Ag nanoparticles exhibited superior anticancer effects compared to ZnO alone [41]. For instance, research on leukemia cell lines demonstrated a lower IC50 value for ZnO-Ag (25 µg/mL) compared to ZnO (50 µg/mL), supporting the notion that the incorporation of silver enhances the therapeutic potential of ZnO nanoparticles. In summary, the present study underscores the potential application of ZnO/Ag nanoparticles as an effective anticancer agent. The combination of oxidative stress induction, mitochondrial dysfunction, and metabolic disruption results in significant cytotoxicity against cancer cells. The utilization of plant-based synthesis further enhances their biocompatibility, making them a promising candidate for further preclinical and clinical evaluations.

Conclusion

In conclusion, ZnO and ZnO/Ag nanoparticles synthesized via *Vicia faba* stem extract showed favorable properties for biomedical use. ZnO/Ag exhibited stronger antibacterial effects, with MIC values down to 58.75 µg/mL for Gram-negative bacteria, compared to 235–940 µg/mL for ZnO. Anticancer activity against A-549 cells also improved

significantly, with ZnO/Ag showing an IC50 of 77.3 versus 165.1 µg/mL for ZnO. This enhancement is attributed to the synergistic antibacterial and cytotoxic mechanisms, including ROS generation and SPR effects. These results highlight their potential for future therapeutic applications.

Acknowledgements We would like to express our sincere gratitude to Cihan University-Erbil and Al-Hadba University for their support and assistance throughout this research project. Their contributions have significantly enhanced the quality of our work and played a crucial role in achieving our research goals.

Author Contribution F.H.A: Investigation, Writing original draft, Methodology; A.A and M.W.M.S: Supervision, Project administration, Methodology; R.A.G and S.A.K: Conceptualization and Formal analysis, M.H.F and A.F.S: Writing original draft and editing the manuscript.

Data Availability No datasets were generated or analysed during the current study.

Declarations

Competing interests The authors declare no competing interests.

References

1. Khojasteh H, Khezri B, Heydaryan K et al (2025) Enhancing Visible Light-Driven Photocatalysis for Water Treatment: Optimizing Fe3O4@SiO2@Cr–TiO2–S Nanocomposite Efficiency with Silver and Palladium Deposition. Plasmonics 20:817–834. https://doi.org/10.1007/s11468-024-02315-3
2. He J, Pan H, Feng L, Feng W (2025) Dual-channel fiber-optic biosensors based on LSPR and SPR for the trace detection of rabies virus. Appl Phys Lett 126. https://doi.org/10.1063/5.0253941
3. Zhao C, Song W, Wang J, Tang X, Jiang Z (2025) Immunoadjuvant-functionalized metal-organic frameworks: synthesis and applications in tumor immune modulation. Chem Comm. https://doi.org/10.1039/D4CC06510G
4. Khanjari Z, Chamani E, Heydaryan K, Mizwari ZM, Salmani F, Farimani AR et al (2024) Unlocking the therapeutic potential: Green synthesized zinc oxide/silver nanoparticles from Sophora pachycarpa for anticancer activity, gene expression analysis, and antibacterial applications. Mater Today Commun 39:109214
5. Ghazi RA, Jasim AS, Heydaryan K, Khojasteh H, Mohammadalizadeh M, Kadhim SA et al (2024) Biosynthesis of Ag-Doped CuO nanoparticles using heracleum persicum extract for enhanced antibacterial and photocatalytic dye degradation properties. Plasmonics 1–12. https://doi.org/10.1007/s11468-024-02298-1
6. Dong Q, Jiang Z (2024) Platinum–iron nanoparticles for oxygen-enhanced sonodynamic tumor cell suppression. Inorganics 12:331
7. Doughty ACV, Hoover AR, Layton E, Murray CK, Howard EW, Chen WR (2019) Nanomaterial applications in photothermal therapy for cancer. Materials 12:779
8. Abdalla AME, Xiao L, Ullah MW, Yu M, Ouyang C, Yang G (2018) Current challenges of cancer anti-angiogenic therapy and the promise of nanotherapeutics. Theranostics 8:533–548
9. Mehra NK, Jain AK, Nahar M (2018) Carbon nanomaterials in oncology: an expanding horizon. Drug Discov Today 23:1016–1025. 2018/05/01/
10. DeLong RK, Cheng Y-H, Pearson P, Lin Z, Coffee C, Mathew EN et al (2019) Translating nanomedicine to comparative oncology—the case for combining zinc oxide nanomaterials with nucleic acid therapeutic and protein delivery for treating metastatic cancer. J Pharmacol Exp Ther 370:671–681. 2019/09/01/
11. Khanam BR, Nidhi MKJ, Nagaraja H, Manjunatha T, Angadi B, Uma Reddy B et al (2024) Physicochemical and therapeutic studies of microwave-synthesized ZnO and Cr-doped ZnO nanoparticles for biomedical applications. Inorg Chem Commun 170:113454. 2024/12/01/
12. Milisav A-M, Mičetić M, Dubček P, Sotelo L, Cantallops-Vilà C, Erceg I et al (2025) Effect of Ag and Cu doping on the properties of ZnO magnetron sputtered thin films for biomedical applications. Appl Surface Sci 690:162623. 2025/05/01/
13. Anjum S, Hashim M, Malik SA, Khan M, Lorenzo JM, Abbasi BH et al (2021) Recent advances in zinc oxide nanoparticles (ZnO NPs) for cancer diagnosis, target drug delivery, and treatment. Cancers (Basel) 13. https://doi.org/10.3390/cancers13184570
14. Yang Y, Xie Y, Liu J, Wang H, Li X, Zhou T et al (2025) Transition metals (Fe/Mn)-doped g-C3N4 and ZnO nanosheet composite sensors for efficient detection of BTEX. Sens Actuat B Chem 428:137251. 2025/04/01/
15. Peksu E, Yener C, Unlu CG, Kulakci M, Karaagac H (2025) Selective synthesis of ZnO nanorods on graphene for solar cell applications. J Alloys Compd 1010:177488. 2025/01/05/
16. Abed SH, Madhi RA, Heydaryan K, Shamkhi AF (2024) Green synthesis of gold-doped ZnFe2O4 nanoparticles using Crataegus monogyna leaf extract: characterization, antibacterial, and efficient degradation of methylene blue and eriochrome black T pollutants. Biomass Convers Biorefin 1–11. https://doi.org/10.1007/s13399-024-05337-3
17. Kiani Z, Mirjalili S, Heydaryan K, Mohammadparast P, Aramjoo H, Bahraini F et al (2024) Harmonizing nature and nanotechnology: phytoextract-mediated synthesis of Ag-doped ZnO nanoparticles using Lavandula stoechas extract for environmental and biomedical applications. J Drug Deliv Sci Technol 96:105708. 2024/06/01/
18. Siami-Aliabad M, Chamani E, Mortazavi-Derazkola S, Khanjari Z, Kiani Z, Aramjoo H et al (2024) Bimetallic S. pachycarpa@Ag-doped ZnO alloy nanoparticles unveil therapeutic promise: revolutionizing multiple myeloma treatment. J Alloys Compd 975:172986. 2024/02/25/
19. Pakdel E, Daoud WA, Wang X (2024) Effect of the photoreduction process on the self-cleaning and antibacterial activity of Au-doped TiO2 colloids on cotton fabric. ACS Appl Mater Interfaces 16:25221–25235. 2024/05/15
20. Ghoreishi SM, Mortazavi-Derazkola S, Mizwari ZM (2024) A dual-function approach for cancer therapy and environmental remediation with advanced photocatalytic, antibacterial, and antioxidant properties: gold-doped zinc oxide nanoparticles. J Nanostruct 14:116–129
21. Jiang C-H, Sun T-L, Xiang D-X, Wei S-S, Li W-Q (2018) Anticancer activity and mechanism of xanthohumol: a prenylated flavonoid from hops (Humulus lupulus L). Front Pharmacol 9:530
22. Kashi MA, Heydaryan K, Khojasteh H, Montazer AH, Eskandari V (2024) Green synthesis of Ag NPs/rGO nanocomposite for use as a non-enzymatic sensor of H2O2. Plasmonics 1–12. https://doi.org/10.1007/s11468-024-02330-4
23. Sahbafar H, Mehmandoust S, Heydaryan K, Zeinalizad L, Abbas MH, Hayder N et al (2023) Surface-enhanced Raman scattering (SERS) and Finite difference time domain (FDTD) investigations of plasmonic and flexible filter papers for the detection of the molecular vibrations of amoxicillin. Plasmonics 1–8. https://doi.org/10.1007/s11468-023-02106-2
24. Heydaryan K, Aspoukeh P, Mehmandoust S, Abbas AH, Khojasteh H, Hadi MS et al (2025) Nanopore/nanocavity-based structures as surface-enhanced Raman spectroscopy (SERS) platforms. Plasmonics 20:1401–1417

25. Aththanayaka S, Thiripuranathar G, Ekanayake S (2025) Comparative Evaluation of the Multifunctional Biological Activities of Palmyra Extract-Mediated Ag/Ag2O, ZnO, and Ag/Ag2O/ZnO Nanomaterials. Waste Biomass Valor 16:847–869. https://doi.org/10.1007/s12649-024-02711-0
26. Nie Y, Li D, Peng Y, Wang S, Hu S, Liu M et al (2020) Metal organic framework coated MnO2 nanosheets delivering doxorubicin and self-activated DNAzyme for chemo-gene combinatorial treatment of cancer. Int J Pharm 585:119513
27. Abed SH, Shamkhi AF, Heydaryan K, Mohammadalizadeh M, Sajadi SM (2024) Sol-Gel Pechini preparation of CuEr2TiO6 nanoparticles as highly efficient photocatalyst for visible light degradation of acid red 88. Ceram Int 50:24096–24102
28. Khojasteh H, Heydaryan K, Aspoukeh P et al (2025) Characterization and Application of CuO Nanoparticles in Gelatin-Glycerol Coatings for Enhanced Shelf Life of Strawberries. Plasmonics 20:803–815. https://doi.org/10.1007/s11468-024-02345-x
29. Katouah HA (2021) Facile synthesis of Co3O4 and ZnO nanoparticles by thermal decomposition of novel Co(II) and Zn(II) Schiff base complexes for studying their biological properties and photocatalytic degradation of crystal violet dye. J Mol Struct 1241:130676. 2021/10/05/
30. Mahmoudi Khatir N, Khorsand Zak A (2024) Antibacterial activity and structural properties of gelatin-based sol-gel synthesized Cu-doped ZnO nanoparticles; promising material for biomedical applications. Heliyon 10:e37022. 2024/09/15/
31. Sun D, Li X, Nie S, Liu J, Wang S (2023) Disorders of cancer metabolism: the therapeutic potential of cannabinoids. Biomed Pharmacother 157:113993
32. Guo Y, Huang C, Pitcheri R, Shekhar B, Radhalayam D, Roy S et al (2025) Bio-green synthesis of bismuth oxide nanoparticles using almond gum for enhanced photocatalytic degradation of water pollutants and biocompatibility. Int J Biol Macromol 300:140222. 2025/04/01/
33. Al-darwesh MY, Babakr KA, Qader IN, Mohammed MA (2025) Antimicrobial, anti-inflammatory, and anticancer potential of green synthesis TiO2 nanoparticles using Sophora flavescens root extract. Chem Papers 79:1207–1221. 2025/02/01
34. Al-darwesh MY, Ibrahim SS, Hamid LL (2024) Ficus carica latex mediated biosynthesis of zinc oxide nanoparticles and assessment of their antibacterial activity and biological safety. Nano-Struct Nano-Objects 38:101163. 2024/05/01/
35. Barzegarparay F, Najafzadehvarzi H, Pourbagher R, Parsian H, Ghoreishi SM, Mortazavi-Derazkola S (2024) Green synthesis of novel selenium nanoparticles using Crataegus monogyna extract (SeNPs@CM) and investigation of its toxicity, antioxidant capacity, and anticancer activity against MCF-7 as a breast cancer cell line. Biomass Convers Biorefin 14:25369–25378. 2024/10/01
36. Al-darwesh MY, Babakr KA, Qader IN (2024) Characterization and anticancer evaluation of zirconia nanoparticles synthesized via green route using sophora flavescens roots extract. Nano-Struct Nano-Objects 39:101245. 2024/09/01/
37. Ghoreishi SM, Mortazavi-Derazkola S (2025) Eco-friendly synthesis of gold nanoparticles via tangerine peel extract: unveiling their multifaceted biological and catalytic potentials. Heliyon 11:e40104. 2025/01/15/
38. Hashemi Z, Mizwari ZM, Alizadeh SR, Habibi M, Mohammadrezaee S, Ghoreishi SM et al (2023) Anticancer and antibacterial activity against clinical pathogenic multi-drug resistant bacteria using biosynthesized silver nanoparticles with Mentha pulegium and Crocus caspius extracts. Inorg Chem Commun 154:110982. 2023/08/01/
39. Kiani Z, Aramjoo H, Mohammadparast P, Bahraini F, Yousefinia A, Nguyen PU et al (2023) Green synthesis of LAE@ZnO/Ag nanoparticles: unlocking the multifaceted potential for biomedical and environmental applications. J Environ Chem Eng 11:111045. 2023/10/01/
40. Zare-Bidaki M, Mohammadparast-Tabas P, Khorashadizade M, Mohammadparast-Tabas P, Alemzadeh , Saberi A et al (2024) Bio-synthesized AGS@AgNPs for wound healing, antioxidant support, antibacterial defense, and anticancer intervention. Biocatal Agric Biotechnol 61:103402. 2024/10/01/
41. Mohammadi-Aghdam S, Bahraini, and S. M. Ghoreishi, In-vitro anticancer on acute lymphoblastic leukemia NALM-6 cell line, antibacterial and catalytic performance of eco-friendly synthesized ZnO and Ag-doped ZnO nanoparticles using Hedera colchica extract. Biomass Convers Biorefin 14:20037–20052 2024/09/01 2024
42. Oualid HA, Essamlali Y, Amadine O, Daanoun K, Zahouily (2017) Green synthesis of Ag/ZnO nanohybrid using sodium alginate gelation method. Ceram Int 43:13786–13790. 2017/11/01/
43. Shirzadi-Ahodashti M, Mizwari ZM, BJafarkhani, Mohamadzadeh S, Abbastabar M, Motafeghi F et al (2022) Biogenic synthesis of spherical-shaped noble metal nanoparticles using Vicia faba extract (X@VF, X = Au, Ag) for photocatalytic degradation of organic hazardous dye and their in vitro antifungal, antibacterial and anticancer activities. Inorg Chem Commun 146:110042. 2022/12/01/
44. Khatami M, Varma RS, Zafarnia N, Yaghoobi H, Sarani M, Kumar VG (2018) Applications of green synthesized Ag, ZnO and Ag/ZnO nanoparticles for making clinical antimicrobial wound-healing bandages. Sustain Chem Pharm 10:9–15. 2018/12/01/
45. Noohpisheh Z, Amiri H, Farhadi S, Mohammadi-gholami A (2020) Green synthesis of Ag-ZnO nanocomposites using Trigonella foenum-graecum leaf extract and their antibacterial, antifungal, antioxidant and photocatalytic properties. Spectrochim Acta Part A Mol Biomol Spectrosc 240:118595. 2020/10/15/
46. Hashem AH, El-Sayyad GS (2024) Antimicrobial and anticancer activities of biosynthesized bimetallic silver-zinc oxide nanoparticles (Ag-ZnO NPs) using pomegranate peel extract. Biomass Convers Biorefin 14:20345–20357. 2024/09/01

Publisher's Note Springer Nature remains neutral with regard to jurisdictional claims in published maps and institutional affiliations.

Springer Nature or its licensor (e.g. a society or other partner) holds exclusive rights to this article under a publishing agreement with the author(s) or other rightsholder(s); author self-archiving of the accepted manuscript version of this article is solely governed by the terms of such publishing agreement and applicable law.